Available online at www.sciencedirect.com
ScienceDirect
Journal of Colloid and Interface Science 321 (2008) 288–293
JOURNAL OF Colloid and Interface Science
www.elsevier.com/locate/jcis

Interaction of DNA bases with silver nanoparticles: Assembly quantified through SPRS and SERS

Soumen Basu, Subhra Jana, Surojit Pande, Tarasankar Pal *

Department of Chemistry, Indian Institute of Technology, Kharagpur 721303, India

Received 2 January 2008; accepted 10 February 2008

Available online 17 March 2008

Abstract

Colloidal silver nanoparticles were prepared by reducing silver nitrate with sodium borohydride. The synthesized silver particles show an intense surface plasmon band in the visible region. The work reported here describes the interaction between nanoscale silver particles and various DNA bases (adenine, guanine, cytosine, and thymine), which are used as molecular linkers because of their biological significance. In colloidal solutions, the color of silver nanoparticles may range from red to purple to orange to blue, depending on the degree of aggregation as well as the orientation of the individual particles within the aggregates. Transmission electron microscopy (TEM), X-ray diffraction (XRD), and absorption spectroscopy were used to characterize the assemblies. DNA base-induced differential silver nanoparticle aggregation was quantified from the peak separation (relates to color) of surface plasmon resonance spectroscopy (SPRS) and the signal intensity of surface-enhanced Raman scattering (SERS), which rationalize the extent of silver–nucleobase interactions.

Keywords: Nucleobase; Surface plasmon; Aggregation; Bathochromic shift

1. Introduction

In recent years, the fabrication of assemblies of perfect nanometer-scale crystallites identically replicated in unlimited quantities is an ultimate challenge in modern materials research because of their outstanding fundamental and potential technological consequences [1]. Since 1996, DNA and its synthetically programmable sequence recognition properties have been utilized to assemble nanoparticles functionalized with oligonucleotides into preconceived architectures [2–5]. These strategies have generated a wide range of architectures with many unusual chemical and physical properties that find innumerable applications due to specificity, programmability, and reproducibility of DNA interactions with nanoparticles [6]. Thus, the nature and strength of interactions of DNA and its components (bases and nucleosides) with metallic nanoparticles are a subject of great interest to researchers in the interdisciplines of nanobiotechnology. The interaction of metal nanoparticles with nucleic acids is topical in the bioinorganic field due to its possible effects on the synthesis, replication, and structural integrity of DNA and RNA [6]. DNA-protected metal nanoparticles, DNA monolayers on metal thin films and electrodes, have a number of diagnostic applications that involve the use of surface-enhanced Raman spectroscopy (SERS), surface plasmon resonance spectroscopy (SPRS), and electrochemical, scanometric, and calorimetric DNA detection strategies [7–9]. The binding modes and conformation of DNA and its components on metal surfaces suggest that the DNA–metal interaction is complex and highly sequence dependent [3,10,11]. It is now well established in the literature that Ag–N affinity is higher than that of Au–N [12]. This serendipitous combination of properties of DNA–metal interactions has encouraged us to find the specificity of silver–nucleobase interactions to provide widespread range of niche applications.

In this paper, we have reported a synthetic strategy for silver nanoparticle/DNA nucleobases and inorganic-biological hybrid nanoassemblies and, thereby, to explore the strength of interaction of the nucleobases with metal surfaces. To the best of our knowledge, this is the first report of organizing silver nanoparticles into periodic functional materials induced by DNA bases

* Corresponding author. Fax: +91 03222 255303.
E-mail address: tpal@chem.iitkgp.ernet.in (T. Pal).

0021-9797/$ – see front matter © 2008 Published by Elsevier Inc.
doi:10.1016/j.jcis.2008.02.015

and to compare the strengths of interactions between the fundamental chemical components of DNA and silver nanoparticle surfaces from surface plasmon resonance spectroscopy and surface-enhanced Raman-scattering signal intensity.

2. Materials and methods

2.1. Reagents and instruments

All the reagents used were of AR grade. Silver nitrate ($AgNO_3$) was purchased from Aldrich. Sodium borohydride, rhodamine B (RB), and all the DNA bases [adenine (A), guanine (G), cytosine (C), and thymine (T)] were obtained from Aldrich Chemicals and used as received. Double-distilled water was used throughout the course of the investigation.

The absorption spectrum of each solution was recorded in a spectrascan UV 2600 digital spectrophotometer (Chemito, India) in a 1-cm well-stoppered quartz cuvette. Transmission electron microscopy (TEM) was carried out on a Hitachi H-9000 NAR transmission electron microscope, operating at 200 kV. Samples were prepared by placing a drop of solution on a carbon-coated copper grid. The X-ray diffraction (XRD) pattern was recorded in an X'pert pro diffractometer with Co ($K\alpha = 1.78891$) radiation. SERS spectra were obtained with a Renishaw Raman microscope, equipped with a He–Ne laser excitation source emitting at a wavelength of 633 nm, and a Peltier cooled (−70 °C) charge-coupled device (CCD) camera. A Leica microscope was attached and was fitted with three objectives (5×, 20×, 50×). For these experiments, the 20× objective was used. Laser power at the sample was 10 mW and the data acquisition time was usually 30 s. The holographic grating (1800 grooves/mm) and the slit enabled a spectral resolution of 1 cm^{-1}. After aggregation of silver particles (⩾3 min) the aqueous solution of RB was introduced and the mixture was kept for 20–30 min. Then a droplet of 20 μl of this solution was spotted on a glass slide to record the SERS spectrum after solvent evaporation. For better results, we have represented the average intensity (average of 5 determinations) in the figures.

2.2. Preparation of silver colloids

Colloidal silver nanoparticles were prepared in an aqueous solution by the reduction of silver nitrate with sodium borohydride following a previous report [13]. Silver sol was prepared by reduction of 1 mM $AgNO_3$ (1 cm^3) with excess ice-cold 2 mM $NaBH_4$ solution (3 cm^3). The solution of silver nitrate was mixed rapidly with vigorous shaking to aid monodispersity. The sol was a yellow color and showed a single visible extinction band near 397 nm (Fig. 1B), characteristic of silver particles substantially smaller than the wavelength of light. The sol was stable and there was no precipitation or change in color on standing for several days.

2.3. Synthesis of DNA base/silver assemblies

Stock solutions of DNA bases (10 mM) were prepared in double-distilled water. Then, an aliquot of any DNA base solution (10 mM, 30 μl) was added to the yellow silver colloidal solution (0.25 mM, 3 ml). The color changed from yellow to blue/green/orange/red, depending on the DNA bases, indicating the formation of the aggregates.

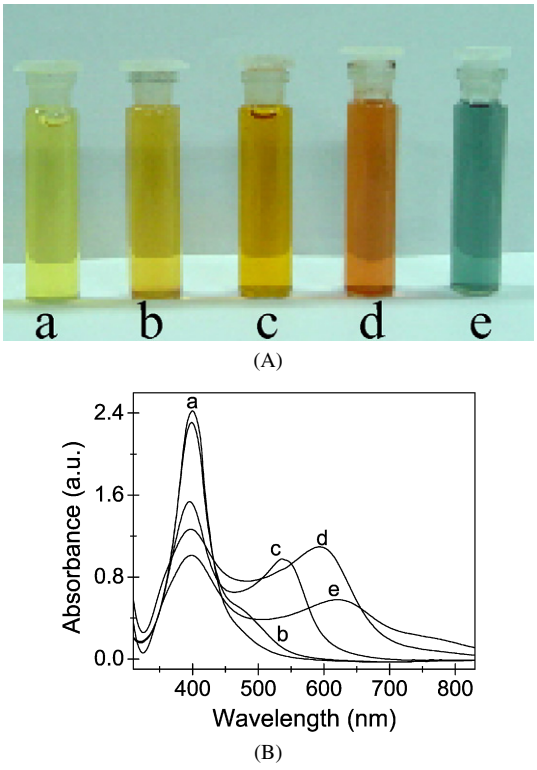

Fig. 1. (A) Photographs of colloidal silver nanoparticles (a, yellow–green) and their aggregates induced by thymine (b, yellow), adenine (c, orange), guanine (d, reddish–green), and cytosine (e, blue–green) measured 3 min after the addition. (B) Corresponding UV–visible spectra.

3. Results and discussion

The reduction of the silver nitrate with borohydride produced a solution of silver nanoparticles with a vivid yellow color, which exhibit an intense surface plasmon absorption band at 397 nm. Following addition of the DNA bases to the silver nanoparticles, the surface plasmon band was shifted to ∼600 nm and a new plasmon band was generated near the resonance peak for single particles [14] at ∼397 nm with sizes 12 ± 2 nm as observed from TEM and the yellow color of the solution was changed to red or orange or blue depending on the different DNA bases, as seen in Fig. 1A. The extent of interaction of the nucleobases with silver nanoparticles is authenticated from different aggregates where the pH remains unchanged (7.0 ± 0.5). A deliberate pH change (4–12) could not bring out any such aggregates. This explains the notion of the study. Fig. 1B shows the typical electronic absorption spectra of the silver nanoparticle aggregates induced by DNA bases. Trace a shows the typical surface plasmon band of spherical silver particles, the origin of which could be traced due to the collective oscillation of the conduction electrons in the totally symmetric geometry of the particles. Following the addition of DNA bases to the silver particles, the surface plasmon band was

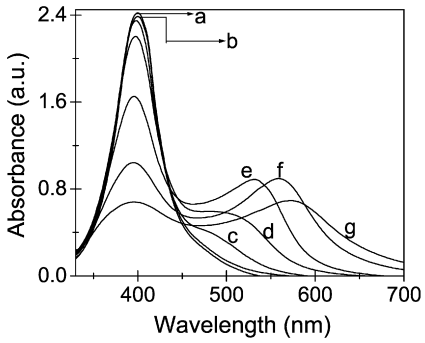

Fig. 2. UV–visible spectra of the aggregates at different concentrations of adenine (a) 0, (b) 10^{-7}, (c) 10^{-6}, (d) 10^{-5}, (e) 10^{-4}, (f) 10^{-3}, and (g) 10^{-2} M measured 3 min after the addition.

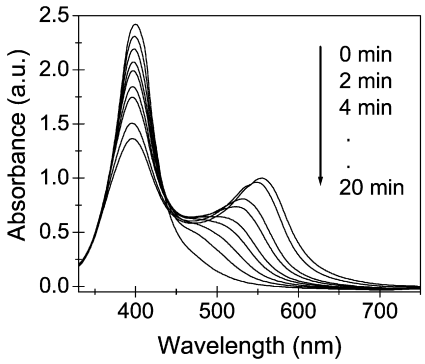

Fig. 3. Time-dependent UV–visible spectra of silver nanoparticles (0.25 mM, 3 ml) recorded at various times after the addition of adenine (1 mM, 30 µl).

shifted near to 600 nm and a new plasmon band was generated near the resonance peak for single particles [14]. Traces b, c, d, and e correspond to the absorption spectra of the nanoscale aggregation of the silver particles on addition of thymine (T), adenine (A), guanine (G), and cytosine (C), respectively. While the first peak, situated near the resonance peak for single particles, could be attributed to the dipole plasmon excitation of the individual silver nanoparticles, the second one at a longer wavelength is assigned to the dipole plasmon resonance appearing due to the aggregation among the individual nanoparticles [14,15]. The appearance of a newly developed extended plasmon band and its relative position with different nucleobases could be accounted for within the framework of effective medium theory [16].

The strength of interaction of the nucleobases with silver surfaces may be evaluated on the basis of the appearance of a clearly defined new peak at longer wavelengths (Fig. 1B). The observed shift could be ascribed to the electromagnetic interactions between the particles that arises when the interparticle spacing is less than five times that of the particle radius ($d \leqslant 5r$) [17]. It is observed that with increasing the concentration of adenine, the intensity of the 397 nm peak gradually decreases and the shoulder peak at ~600 nm dominates. It was noted that the aggregation occurs above a threshold concentration of adenine and at a very high concentration, the particles precipitated (Fig. 2). From this, it can be inferred that [Ag]:[nucleobase] plays a role in inducing the aggregation among the silver particles. Kinetic studies employing a particular nucleobase reveal a progressive red shift of the dipole plasmon resonance from 397 to 600 nm accompanied by a generation of dipole plasmon resonance at 397 nm, indicating the decrease in interparticle spacing with the progress of the reaction (Fig. 3). From the overall bathochromic shift of λ_{max} in the absorption spectra, it is clear that the strength of interaction of the nucleobases with silver nanoparticles is in the order C > G > A > T. In cytosine the available lone pair from exocyclic nitrogen takes part in binding silver. It can generate a lesser amount of canonical structures than guanine and adenine. So Ag nanoparticles would strongly interact with cytosine. Thymine has no such exocyclic nitrogen. So, the interaction would be least in this case. Between guanine and adenine the exocyclic nitrogen in guanine is adjacent to two almost equivalent ring nitrogens in

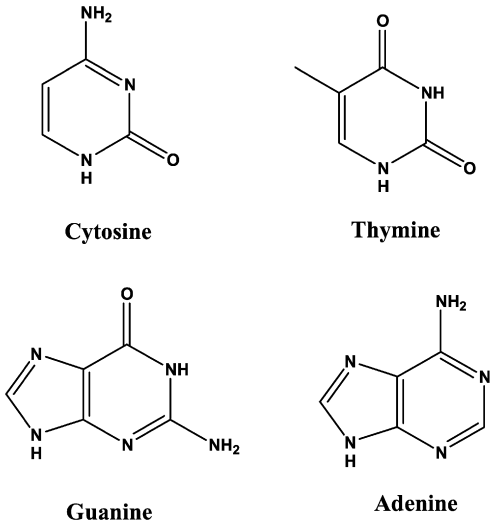

Scheme 1. Structure of the DNA bases.

its six-membered skeleton which might be the reason for better interaction with Ag nanoparticles. Recent DFT and Post Hartree-Fock calculations have shown that the interaction of the DNA bases with the gold surface is dominated by dispersion interactions [18]. As the strength of the interaction between the silver–nucleobase increases, the interparticle spacing between the particles decreases and this is reflected by the position of the extended plasmon band of the colloids. The difference in strength of interaction is likely due to the varying ability of the bases to coordinate the nanoparticle surface as a result of the different types of possible surface binding moieties and these possible nonspecific chemical interactions result in different aggregation mechanisms for different nucleobases. It is well established in the literature that amines can bind exceptionally strongly with silver nanoparticles [12]. Therefore, it is reasonable to believe that the weakest interaction of thymine with the silver nanoparticles is due to the absence of an exocyclic amine group in this nucleobase (structures of the nucleobases are shown in Scheme 1). The weakest interaction of thymine is in agreement with previous results [19–21] (C > G > A > T) while Sastry and co-workers [19] have used isothermal titration calorimetry to study the interaction of DNA bases and PNA bases with gold nanoparticles.

For a better comparison, the adsorption kinetics of the nucleobases was monitored by the growth of surface plasmon band at 650 nm [5]. As expected the DNA bases C, G, and A exhibited a much faster growth kinetics than T under the same experimental conditions (Fig. 4). This indicates that the DNA bases C, G, and A have a higher binding affinity for the silver nanoparticle surface than T.

Figs. 5A, 5B, 5C, and 5D show the TEM images of the aggregates of silver nanoparticles due to the addition of DNA bases C, G, A, and T, respectively. Although the apparent variation of the size and shape in the TEM images are unable to highlight the differential binding affinities among the nucleobases, the tailorability of the optical properties using this assembling strategy is indeed achievable through the use of DNA base interconnects. The UV–visible spectrum and SERS are the authentic and real-time proof for base-induced aggregation. TEM just supports the observed phenomenon and this is not a real-time measurement. From XRD analysis (Fig. 6), the diffraction peaks at $2\theta = 44.5$, 51.7, 76.5, 92.8, and 97.8° are indexed as (111), (200), (220), (311), and (222) planes of fcc of

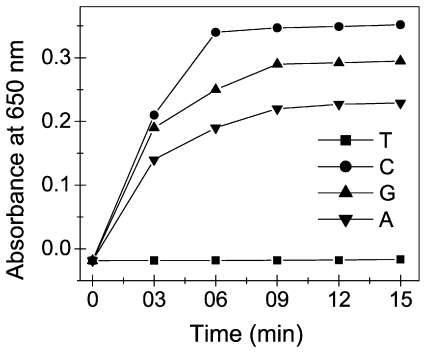

Fig. 4. Absorbance (at 650 nm) vs time plot for silver particle aggregation by different nucleobases.

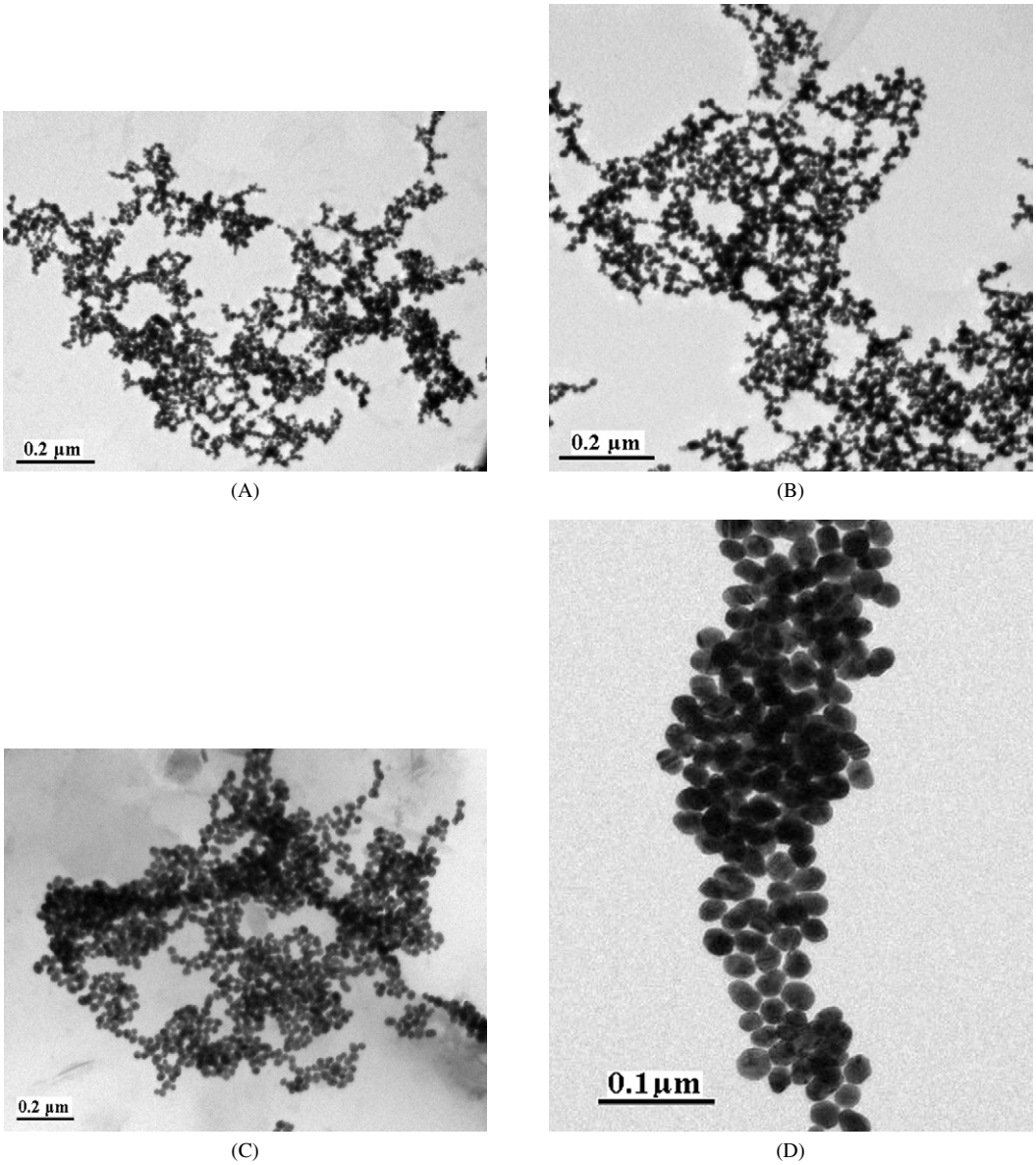

Fig. 5. TEM images of silver aggregates with (A) cytosine, (B) guanine, (C) adenine, and (D) thymine.

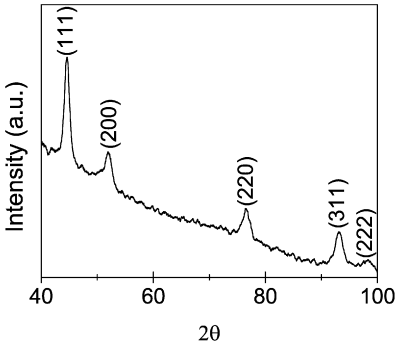

Fig. 6. X-ray diffraction pattern of silver aggregates induced by cytosine.

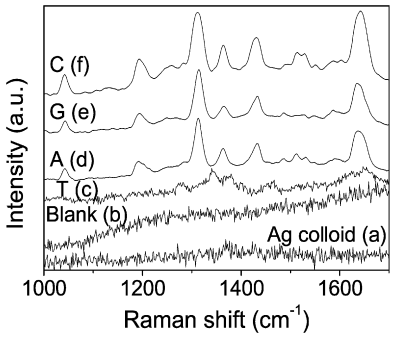

Fig. 7. Normalized (to 1307 cm^{-1}) SERS spectra of 10^{-7} M RB for different DNA base-induced silver aggregates (c–f), normal Raman spectra of silver colloid (a), and blank RB at 10^{-7} M (b).

of the cubic silver phase. The observation of diffraction peaks for the silver nanoparticles indicates that these are crystalline in this size range while their broadening is related to the reduced particle size.

Since the discovery of SERS, silver nanoparticles with roughened surfaces has been found to be the best-suited substrate for measurements as the dielectric constant of silver near the Fröhlich frequency gives rise to intense plasmon absorption in the visible region [22,23]. Aggregation among the metal particles offers a strong influence on SERS because rough or fractal surfaces can give rise to a stronger coupling of the electric field that happen to be resonantly excited by the illuminating laser are called "hot spots" [24,25]. We have employed an aqueous solution of rhodamine B as a Raman probe to correlate the morphology and electronic absorption spectra with the enhancement patterns observed in the SERS spectra. No internal standard was used as we are comparing the differently aggregated silver sol system only with the same probe molecules (10^{-7} M). Foreign substances such as "acetone" as an internal standard substance change the aggregation of the silver sol system. So our intention to quantify the "strength of interaction" of DNA bases with silver nanoparticles gets lost. Fig. 7 shows the SERS spectra (1000–1700 cm^{-1}) of RB adsorbed on the silver aggregates induced by different nucleobases. Spectrum a is the Raman spectrum of Ag colloid without RB. The concentration of the probe, RB in these studies, is kept at 10^{-7} M. At this concentration no normal Raman signal is observed (spectrum b, Fig. 7) in the absence of the colloidal silver under the same experimental conditions. Spectra c–f show SERS effects

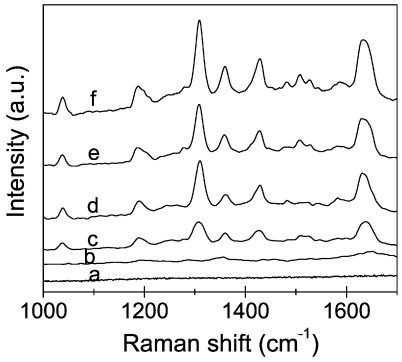

Fig. 8. Successive increases in the SERS intensity of RB at the different stages of aggregation of silver nanoparticles using adenine at definite time intervals: (a) 0 min, (b) 2 min, (c) 4 min, (d) 8 min, (e) 10 min, and (f) 12 min.

of RB molecules adsorbed on the DNA base aggregated silver nanoparticle surfaces. It was observed that the SERS-enhanced signal intensities are different for different DNA bases with a constant dye concentration (10^{-7} M) and without the need for any extra activating agent. Here the surface of each aggregate and, therefore, the orientation of the molecular probes in the proximity of the metal surfaces are different. This changes the orientation of the probe molecule to show different SERS signal intensities. As the SERS intensity increases in the order T < A < G < C, it can be concluded that the strength of interaction of the nucleobases is in the order C > G > A > T.

Vibrational spectroscopy revealed that weakly polarizable single bonds of the sugar derivatives of different nucleosides remain indifferent and do not take part in binding metal surfaces. Hence we considered the DNA nucleobases only to study their effects to bring forth the aggregates of silver nanoparticles. In turn the aggregates have been shown to be efficient substrates for SERS studies. Under the experimental conditions, the nucleobases do not adsorb efficiently with the metal surfaces to cause SERS enhancement to a meaningful extent. Thus, we have selected RB as a probe. From the SERS results and Ref. [21], it is proposed that the best aggregation of silver particles takes place where stronger interactions prevail with nucleobases. Thus, we could compare the extent of aggregation which follows the order C > G > A > T. In the case of T presumably ring nitrogen does not take part in bonding. Hence the orientation of the molecular plane becomes perpendicular to the surface of silver particles instead of being parallel as in the other three cases [21]. The best aggregation takes place in the case of C as nitrogen and oxygen become preferred donors. On the other hand, enolisation of the >C=O functionality might help a stronger interaction for G which produces better aggregates than those obtained for A.

In the electromagnetic description of SERS, the enhancement is caused by an amplification of the electric field due to the response of the material and the coupling between different surfaces. The enhancement of the local field can vary by several orders of magnitude. Fig. 8 shows the normalized (to 1307 cm^{-1}) SERS spectra of RB obtained from silver particles at different stages of aggregation. The enhancement is observed for xanthene ring deformation at 427 cm^{-1}, C–C–C

ring in plane bending at 625 cm^{-1}, C–H out of plane bending at 740 cm^{-1}, C–O–C stretching at 1307 cm^{-1}, xanthene ring stretching at 1360, 1579, and 1638 cm^{-1}, and external phenyl ring stretching at 1506 cm^{-1}. It was observed that the SERS intensity increases as the interparticle distance between the silver aggregates decreases with a constant dye concentration. It can be seen from Fig. 3 that the surface plasmon peak gradually red-shifted with time, indicating the decrease in interparticle separation. A red-shifted plasmon band indicates that the size of the aggregate also increases. As the size of the aggregate increases, the number of "hot junctions" increases and thus provides a much more intense SERS band. From this result, we can conclude that the enhancement was due to an electromagnetic effect. Since, in this study, there is no need to add any extra aggregating agent, we can conclude that the electromagnetic field enhancement plays the major role. The SERS signal varies significantly from spot to spot due to the presence of hot spots in the aggregate structures and a variation of 7% signal intensity was observed. So we have indicated an average effect of the SERS signal in Figs. 7 and 8.

4. Summary

In conclusion, silver particle aggregation caused by different DNA bases is substantiated primarily from SPRS peak separation and finally from SERS signal intensity. The interparticle distance in silver aggregates changes with different interacting DNA bases that caused SERS enhancement. This has been reported for the first time. The strength and extent of interaction of different DNA bases with spherical silver colloids bearing a tight size distribution unequivocally speak for the successive enhancement due to a high electromagnetic field. Nucleobases are the molecular building blocks of DNA that may be involved in base pairing. So to study the interaction of the nucleobases with nanoparticles is important. This is a preliminary work in a study of their interactions with nanoparticles. Later we will apply this system to identify the level-free DNA bases in aqueous solution with the help of SPRS and SERS. The field of biochip technology and therapeutic applications may gain a new momentum, taking the variable strength of interactions into consideration.

Acknowledgments

The authors are thankful to IIT Kharagpur, DST, CSIR, and UGC, New Delhi, for financial assistance. We are thankful to both reviewers for suggestions and constructive comments.

References

[1] I. Willner, E. Katz, Angew. Chem. 43 (2004) 6042.
[2] C.A. Mirkin, R.L. Letsinger, R.C. Mucic, J.J. Storhoff, Nature 382 (1996) 607.
[3] A.B. Steel, T.M. Herne, M.J. Tarlov, Anal. Chem. 70 (1998) 4670.
[4] L. He, M.D. Musick, S.R. Nicewarner, F.G. Salinas, S.J. Benkovic, M.J. Natan, C.D. Keating, J. Am. Chem. Soc. 122 (2000) 9071.
[5] J.J. Storhoff, R. Elghanian, R.C. Mucic, C.A. Mirkin, R.L. Letsinger, J. Am. Chem. Soc. 120 (1998) 1959.
[6] H. Colfen, S. Mann, Angew. Chem. 42 (2003) 2350.
[7] D. Graham, W.E. Smith, A.M.T. Linacre, C.H. Munro, N.D. Watson, P.C. White, Anal. Chem. 69 (1997) 4703.
[8] K.A. Peterlinz, R.M. Georgiadis, T.M. Herne, M.J. Tarlov, J. Am. Chem. Soc. 119 (1997) 3401.
[9] L.M. Demers, C.A. Mirkin, R.C. Mucic, R.A. Reynolds III, R.L. Letsinger, R. Elghanian, G. Viswanadham, Anal. Chem. 72 (2000) 5535.
[10] B. Thomas, D.R. Buddy, Langmuir 10 (1994) 3845.
[11] N.J. Tao, J.A. DeRose, S.M. Lindsay, J. Phys. Chem. 97 (1993) 910.
[12] S. Nath, S.K. Ghosh, S. Kundu, S. Praharaj, S. Panigrahi, T. Pal, J. Nanopart. Res. 8 (2006) 111.
[13] J.A. Creighton, C.G. Blatchford, M.G. Albrecht, J. Chem. Soc. Faraday Trans. 75 (1979) 790.
[14] T. Jensen, L. Kelly, A. Lazarides, G.C. Schatz, J. Cluster Sci. 10 (1999) 295.
[15] S.K. Ghosh, T. Pal, Chem. Rev. 107 (2007) 4797.
[16] J.C. Maxwell-Garnett, Philos. Trans. R. Soc. 203 (1904) 805.
[17] S. Basu, S. Panigrahi, S. Praharaj, S.K. Ghosh, S. Pande, S. Jana, T. Pal, New J. Chem. 30 (2006) 1333.
[18] S. Piana, A. Bilic, J. Phys. Chem. B 110 (2006) 23467.
[19] A. Gourishankar, S. Shukla, K.N. Ganesh, M. Sastry, J. Am. Chem. Soc. 126 (2004) 13186.
[20] L.M. Demers, M. Ostblom, H. Zhang, N.H. Jang, B. Liedberg, C.A. Mirkin, J. Am. Chem. Soc. 124 (2002) 11248.
[21] N.H. Jang, Bull. Korean Chem. Soc. 23 (2002) 1790.
[22] A.M. Michaels, M. Nirmal, L.E. Brus, J. Am. Chem. Soc. 121 (1999) 9932.
[23] H. Kneipp, J. Kneipp, K. Kneipp, Anal. Chem. 78 (2006) 1363.
[24] H. Xu, J. Aizpurua, M. Kall, P. Apell, Phys. Rev. E 62 (2000) 4318.
[25] H. Xu, E.J. Bjerneld, M. Kall, L. Borjesson, Phys. Rev. Lett. 83 (1999) 4357.